Damage generation and removal in the Ga^+ focused ion beam micromachining of GaN for photonic applications

Irving Chyr, Boon Lee, L. C. Chao, and A. J. Steckl[a)]
Nanoelectronics Laboratory, University of Cincinnati, Cincinnati, Ohio 45221-0030

(Received 1 June 1999; accepted 18 August 1999)

We have investigated focused ion beam (FIB) micromachining of GaN films with the goal of fabricating distributed Bragg reflection air/GaN gratings for short cavity lasers. The FIB micromachining process creates damage in the GaN film. To reduce the damage evidenced in the GaN photoluminescence (PL) spectrum, we utilized both furnace annealing for 1 h and rapid thermal annealing (RTA) from 10 to 50 s at 1050 °C. Pulsed nitrogen and He–Cd lasers have been utilized as excitation sources to study differences in the PL spectra from the FIB-milled distributed Bragg reflector (DBR) gratings and the nonmilled GaN film. Surface roughness does not change with increasing annealing time of RTA. The threshold pumping condition has been investigated to compare the DBR grating area with as grown GaN film. We found that the threshold pumping intensity for these two conditions are almost the same, i.e., FIB micromachining followed by thermal anneal would not degrade the PL spectrum performance of GaN film. © *1999 American Vacuum Society.* [S0734-211X(99)08906-4]

I. INTRODUCTION

GaN and its related alloy of III–nitride materials have had great success in the fabrication of light emitting devices such as light emitting diodes[1,2] and laser diodes.[3] In order to increase the optical pumping efficiency of GaN and related materials, two methods can be used: (1) increase in photoluminescence (PL) efficiency by improved growth techniques and/or thermal annealing such as rapid thermal annealing (RTA);[4–6] (2) increase in mirror reflectivity. Currently, the mirror facets of laser diodes fabricated using GaN-based structures are formed by either the cleaving method[7] or by plasma etching.[8] Due to a combination of substrate and process issues, both conventional methods do not provide a simple and efficient processing technique for producing low mirror loss and mode selection of laser diodes. Recently, several research groups[9–12] reported an alternative method to enhance the mirror reflectivity of semiconductor lasers by introducing a short stack distributed Bragg reflector (DBR) grating consisting of multilayers of semiconductor materials and air. This is very interesting since the large refractive index difference between semiconductor materials and air provides a very high reflectivity and allows for the reduction of the length of cavity.

The focused ion beam (FIB) technique is a useful tool for many aspects of photonic and microelectronic device fabrication. Recently, FIB has been applied to GaN for micromachining of flat and smooth mirror facets for laser diodes[13–15] and for implanting rare earth elements which have resulted in localized visible and infrared PL emission.[16] We have previously reported[17,18] the micromachining and sputtering yields of GaN and related substrate materials utilizing Ga^+ and Au^+ FIB micromachining. In this article, we present the results of thermal annealing and threshold emission condition from DBR grating structures fabricated by FIB micromachining.

II. EXPERIMENT

A Ga^+ liquid metal ion source was used in the NanoFab 150 FIB system. The FIB micromachining conditions and system configuration have been previously reported.[16] The GaN samples for this study were grown on sapphire substrates using either metallorganic chemical vapor deposition (MOCVD) system and hydride vapor phase epitaxy (HVPE). The thicknesses of the MOCVD and HVPE GaN films are 2 and 20 μm, respectively.

The MOCVD sample was subjected to a series of sequential 10 s anneals at 1050 °C in a N_2 ambient. The HVPE GaN sample was annealed in Ar for 1 h at the same temperature. Both GaN samples were annealed without a surface cover. The GaN surface was characterized by atomic force microscopy (AFM) prior to any processing and then again after each anneal. A Digital Instrument Dimension 3100 AFM was used in the tapping mode to take a 3 μm×3 μm image at each annealing step. Each image was analyzed for the surface roughness.

PL measurements were performed on the GaN samples at room temperature using pulsed N_2 and cw He–Cd lasers. The pulsed N_2 laser (337.1 nm) operated with a repetition rate of 5 Hz, a nominal energy of 1.45 mJ per pulse, and a pulse duration of 0.6 ns. The He–Cd laser (325 nm) has a nominal emitted power of 60 mW. The laser beams were focused on the sample surface through an optical microscope, resulting in a rectangular beam shape for the N_2 laser of about 300×100 μm^2 and an approximately circular beam for the He–Cd laser with a diameter of about 20 μm. The emitted spectrum signal from the GaN sample was measured with a monochromator. A photomultiplier and a lock-in amplifier were used to enhance the optical signal-to-

[a)]Electronic mail: a.steckl@uc.edu

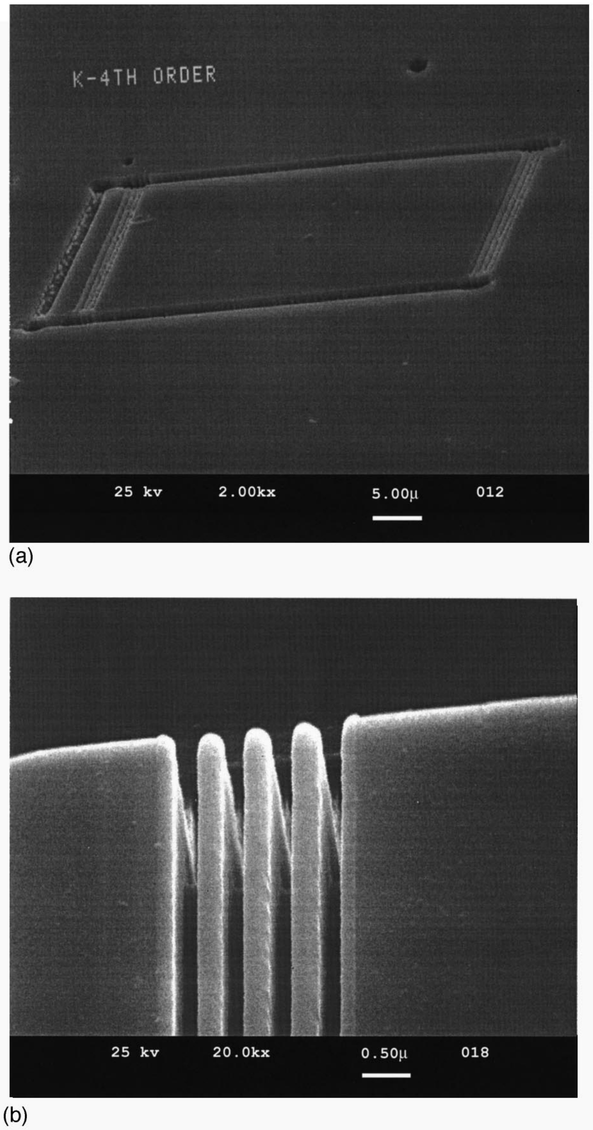

FIG. 1. SEM photographs of MOCVD GaN short cavity laser with DBR gratings fabricated by FIB micromachining: (a) overview of laser structure, cavity length is ~50 μm; (b) fourth order grating structure, the period is 500 nm and spacing is 150 nm.

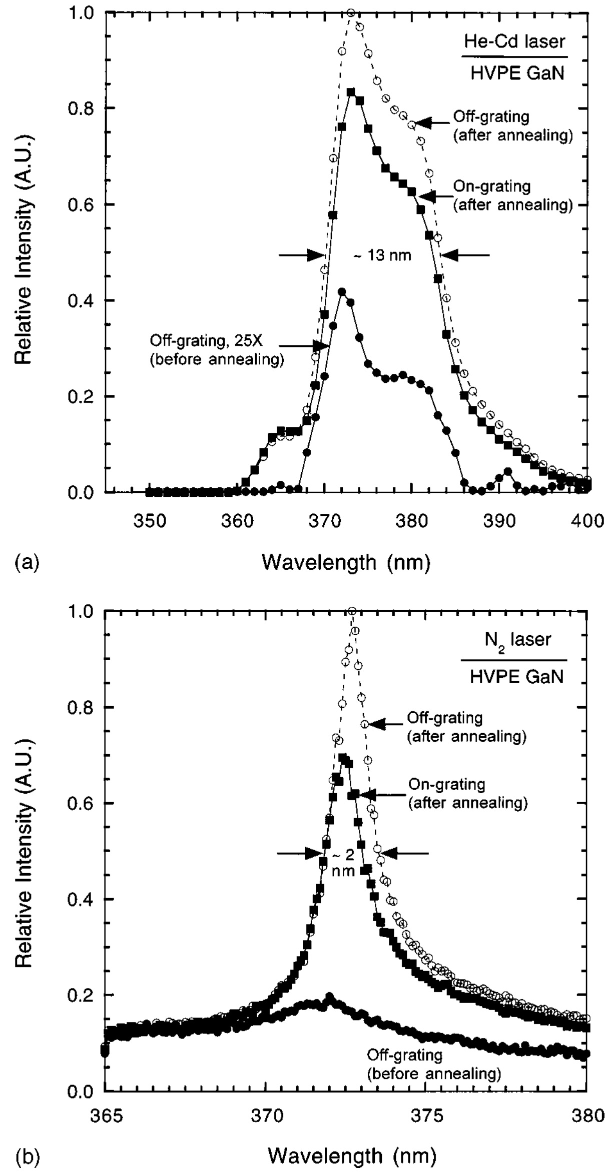

FIG. 2. Photoluminescence spectra of HVPE GaN sample (total cavity length of ~70 μm) before and after furnace annealing at 1050 °C and 1 h for off-grating and on-grating areas: (a) He–Cd laser pumping; (b) N_2 laser pumping.

noise ratio in order to allow measurement of small signals from the GaN films.

III. RESULTS

The cavity and DBR gratings were fabricated with the same experimental conditions as described previously.[17] In Fig. 1, we show scanning electron microscope (SEM) photographs of the DBR gratings and short cavity laser structure fabricated in GaN by Ga^+ ion FIB micromachining. The SEM photographs were taken with the sample tilted at an angle of 60° from the horizontal. The dimensions of the cavity are 70 μm by 20 μm, as shown in Fig. 1(a). The DBR structure shown in Fig. 1(b) is a fourth order grating, which was designed for a lasing wavelength of 370 nm, with a period of 500 nm, and spacing of 150 nm. The depth of the DBR grating is close to 2 μm. On the sidewalls of waveguides and DBR grating, there are occasionally some tiny Ga droplets, which can be removed by dipping in an HCl solution. The redeposition effect in our experiments appears negligible when we utilized multiple serpentine FIB scans.[17] The SEM photographs demonstrate that FIB is a very accurate technique for the fabrication of DBR gratings and related optoelectronic and photonic devices in GaN.

In Figs. 2(a) and 2(b), we compare the He–Cd and N_2 PL spectra of the HVPE GaN sample before and after furnace annealing. The PL spectra reveal that the emission efficiency of as-grown GaN (''off-grating'' area) is enhanced by the furnace anneal. The off-grating area is chosen several hundred micrometers away from the structures of cavity and DBR gratings to avoid the possible perturbation by the beam tail of the FIB. The off-grating PL signals after annealing are

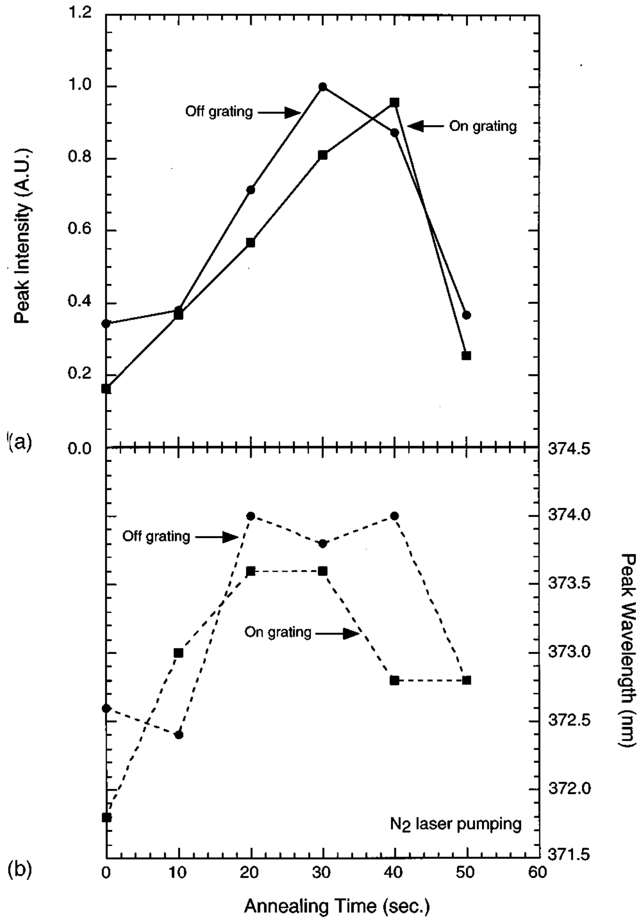

FIG. 3. Comparison of off-grating and on-grating areas as a function of rapid thermal annealing time for N_2 laser pumping in MOCVD GaN sample in: (a) peak intensity; (b) peak wavelength.

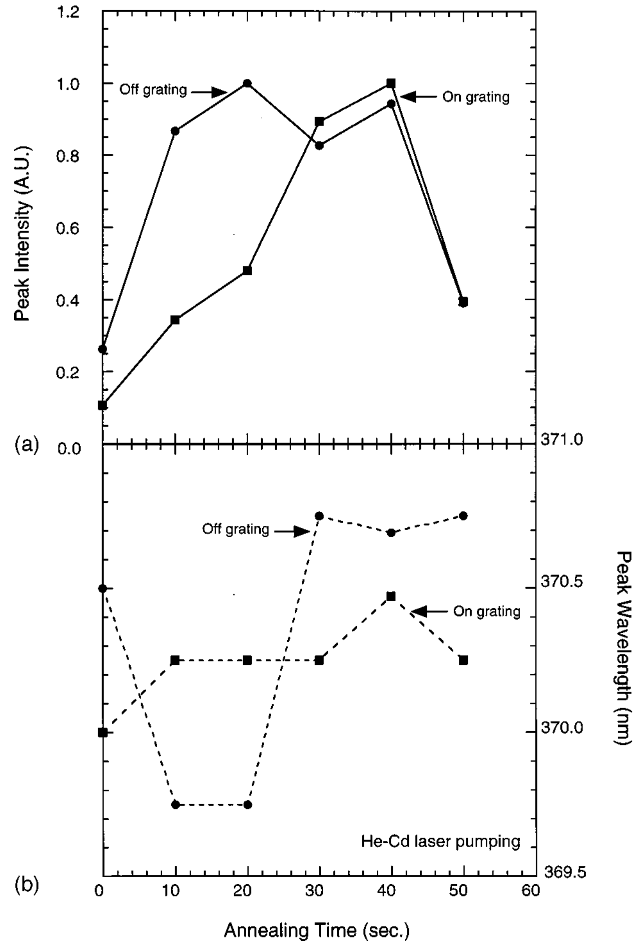

FIG. 4. Comparison of off-grating and on-grating areas as a function of rapid thermal annealing time for He–Cd laser pumping in MOCVD GaN sample in: (a) peak intensity; (b) peak wavelength.

seven and 60 times larger for N_2 and He–Cd laser pumping than before annealing. The on-grating area is a region that includes the cavity and the DBR gratings. The PL spectrum of the on-grating area for the N_2 laser pumping covered the entire cavity area and the adjacent region, while for He–Cd laser pumping the beam covered the center of the cavity. Therefore, the PL spectra of the on-grating area can readily indicate the effects of the ion damage induced from FIB micromachining. The on-grating PL spectrum before furnace anneal was extremely small and is not shown in Fig. 2. However, after the HVPE GaN sample was treated by a high temperature thermal effect, the on-grating PL spectrum is quite close in magnitude to that of the off-grating area. This indicates that the furnace annealing was very efficient in recovering the damage produced by FIB micromachining. Nonetheless, we need to explore in more detail the influence of FIB micromachining on the optical characteristics of actual photonic devices.

Figures 3 and 4 contain the PL peak intensity and peak wavelength in the MOCVD GaN sample as the function of rapid thermal annealing time under N_2 and He–Cd laser excitation. We consider first the case of pulsed N_2 laser pumping. In Fig. 3(a), the PL peak intensity increases nearly linearly with annealing time from 10 to 40 s for both off-grating and on-grating areas. In both areas, the PL intensity drops significantly after the final anneal at a total of 50 s to a level close to the level before annealing. In Fig. 3(b), the peak wavelength change with annealing time shows a similar behavior: first an increase of ~2–3 nm after the first 20–30 s, followed by a decline back to the values only slightly higher than those obtained prior to any anneal. This behavior is observed for PL from both on- and off-grating areas.

Turning to the case of He–Cd laser pumping, we observed a similar phenomenon with regard to the PL peak intensity versus anneal time, as shown in Fig. 4(a). After the first 20–30 s of annealing, the PL peak intensity increases 4–6 times the unannealed levels for both the off-grating and on-grating areas. After 50 s cumulative annealing time, the PL of both areas drops to a level close to the initial peak intensity level. The peak wavelength versus anneal time behavior is somewhat different for He–Cd vs N_2 laser pumping. The on-grating peak wavelength follows a generally, but slightly increasing trend with anneal time, while the off-grating peak wavelength undergoes both positive and negative swings. It is interesting to point out that there is ~2 nm difference in the peak wavelength of the as-grown case for the two excitation sources. From the data of Figs. 3 and 4,

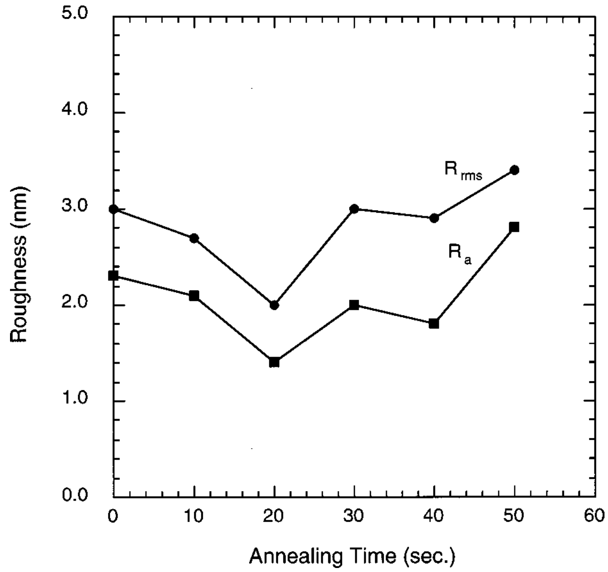

FIG. 5. Surface roughness vs rapid thermal annealing time for MOCVD GaN sample.

we can conclude that the material quality of both off-grating and on-grating areas is improved by the rapid thermal annealing time up to ~30–40 s. After the GaN sample was treated up to 50 s, the thermal effect degrades the PL efficiency to the case of no RTA.

Figure 5 shows the evolution of the surface roughness of the MOCVD GaN sample with RTA time in N_2 ambient at 1050 °C. The definition of rms roughness is the standard deviation of the surface values within a given area and mean roughness is the mean value of the surface relative to the center plane. The roughness of the as-grown sample is ~2.0–3.0 nm. After RTA processing, the surface roughness of the annealed sample is only slightly changed with the increase of anneal time. Large particles are found on the surface of the GaN sample after the 50 s anneal. The effect of these particles is removed from the estimate of surface roughness. It is possible that these particles are Ga droplets formed because of GaN dissociation during the high temperature annealing process.

We have investigated PL emission spectrum as a function of N_2 laser pump intensity for on-grating and off-grating area of the annealed HVPE GaN sample. We used glass slides to reduce the pumping power of the pulsed N_2 laser. As can be seen in Fig. 6, the output signal power increases greatly with the pumping power after a certain threshold is exceeded. At the same time, the emission spectra of output power appear to shift to longer wavelength. Beyond the threshold condition, the full width half maximum of the 372 nm emission is reduced to 1.7 from 2.9 nm for the off-grating area and to 2.4 from 4.2 nm for on-grating area. The data of peak emission intensity versus pumping intensity for the off-grating and on-grating areas are plotted in Fig. 7. The emission signals of the off-grating area are slightly larger than those of the on-grating area. We observed that both cases have nearly identical threshold condition, even though we expected that the DBR gratings would enhance the stimulated emission of GaN films. This observation is similar to the conclusion of Khan *et al.*[19] They claimed that the stimulated emission was from the single shot emission due to the high pumping power of the N_2 laser.

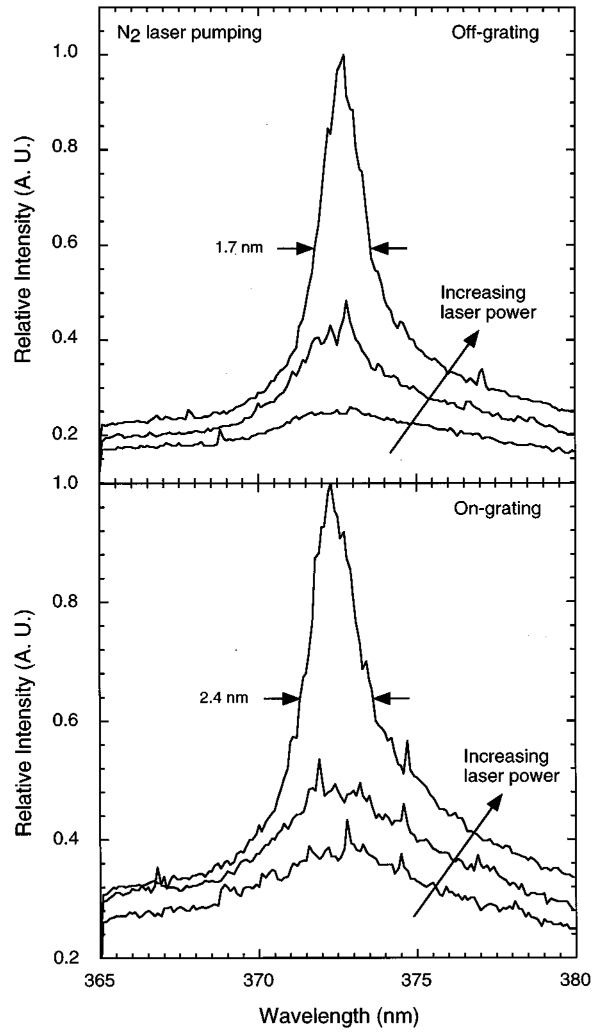

FIG. 6. Stimulated emission spectra as a function of N_2 laser pumping intensity for off-grating and on-grating areas in furnace annealed HVPE GaN sample.

IV. CONCLUSION

In conclusion, we have reported the fabrication for DBR gratings and short cavity lasers by Ga^+ FIB micromachining. We have measured the PL spectra of HVPE and MOCVD GaN samples by pulsed N_2 and He–Cd lasers for off-grating and on-grating areas. We have observed that the peak intensity and peak wavelength of both areas are linearly dependent on the RTA time. However, the peak intensity and peak wavelength of both areas reduce their values close to the level of the as-grown GaN sample after a total of 50 s anneal time. The surface roughness of GaN films is slightly changed with the increase of anneal time. The threshold for the stimulated emission condition of off-grating and on-grating areas

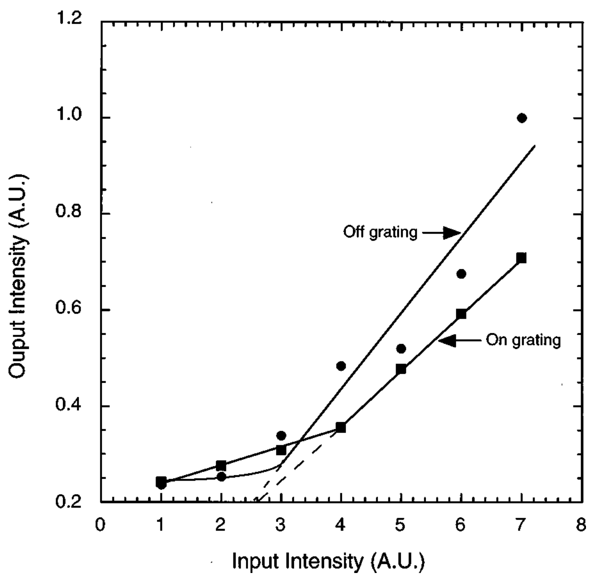

FIG. 7. Threshold emission condition of N_2 laser pumping intensity for off-grating and on-grating areas in furnace annealed HVPE GaN sample.

shows that the processing of FIB micromachining does not degrade the optical performance of GaN samples after thermal annealing effect.

ACKNOWLEDGMENTS

The authors gratefully acknowledge the discussion for the setup of optical characterization with Dr. D. A. Stocker from Photonics Research Center of Boston University. This work was supported by an MRL-DOD grant.

[1]V. E. Kudryashov, K. G. Zolin, and F. I. Manyakhin, Semiconductors **31**, 1123 (1997).
[2]N. Grandjean, J. Massies, and P. Lorenzini, Appl. Phys. Lett. **72**, 82 (1998).
[3]S. Nakamura, T. Mukai, and M. Senoh, Appl. Phys. Lett. **64**, 1678 (1994).
[4]J. C. Zolper, M. H. Crowford, and A. J. Howard, Appl. Phys. Lett. **68**, 200 (1996).
[5]J. Hong, J. W. Lee, C. B. Vartuli, C. R. Abernathy, J. D. MacKenzie, S. M. Donovan, S. J. Pearton, and J. C. Zolper, J. Vac. Sci. Technol. B **15**, 797 (1999).
[6]N. I. Katsavets, G. M. Laws, I. Harrison, E. C. Larkins, T. M. Benson, T. S. Cheng, and C. T. Foxon, Semiconductors **32**, 1048 (1998).
[7]M. A. Khan, D. T. Olson, J. M. Van Hove, and J. N. Kuznia, Appl. Phys. Lett. **58**, 1515 (1991).
[8]F. Binet, J. Y. Duboz, N. Laurent, C. Bonnat, P. Collot, F. Hanauer, O. Briot, and R. L. Aulombard, Appl. Phys. Lett. **72**, 960 (1998).
[9]T. Baba, M. Hamasaki, N. Watanabe, P. Kaewplung, A. Matsutani, T. Mukaihara, F. Koyama, and K. Iga, Jpn. J. Appl. Phys., Part 1 **35**, 1390 (1996).
[10]Y. Yuan, T. Brock, P. Bhattacharya, C. Caneau, and R. Bhat, IEEE Photonics Technol. Lett. **9**, 881 (1997).
[11]T. F. Krauss, O. Painter, A. Scherer, J. S. Roberts, and R. M. De La Rue, Opt. Eng. (Bellingham) **37**, 1143 (1998).
[12]E. Hofling, R. Werner, F. Schafer, J. P. Reithmaier, and A. Forchel, Electron. Lett. **35**, 154 (1999).
[13]T. Ito, H. Ishikawa, T. Egawa, T. Jimbo, and M. Umeno, Jpn. J. Appl. Phys., Part 1 **36**, 7710 (1997).
[14]H. Katoh *et al.*, Jpn. J. Appl. Phys., Part 2 **36**, L444 (1998).
[15]M. P. Mack, G. D. Via, A. C. Abare, M. Hansen, P. Kozodoy, S. Keller, J. S. Speck, U. K. Mishra, L. A. Coldren, and S. P. DenBaars, Electron. Lett. **34**, 1315 (1998).
[16]L. C. Chao and A. J. Steckl, Appl. Phys. Lett. **74**, 2364 (1999).
[17]A. J. Steckl and I. Chyr, J. Vac. Sci. Technol. B **17**, 362 (1999).
[18]I. Chyr and A. J. Steckl, MRS Internet J. Nitride Semicond. Res. **4S1**, G10.7 (1999).
[19]M. A. Khan, D. T. Olson, J. M. Van Hove, and J. N. Kuznia, Appl. Phys. Lett. **58**, 1515 (1999).